ACS NANO

www.acsnano.org

ARTICLE

A Hydrophobic Self-Repairing Power Textile for Effective Water Droplet Energy Harvesting

Cuiying Ye,[δ] Di Liu,[δ] Xiao Peng,[δ] Yang Jiang, Renwei Cheng, Chuan Ning, Feifan Sheng, Yihan Zhang, Kai Dong,* and Zhong Lin Wang*

Cite This: *ACS Nano* 2021, 15, 18172−18181

Read Online

ACCESS | Metrics & More | Article Recommendations | Supporting Information

ABSTRACT: **Triboelectric nanogenerators (TENGs) are useful for harvesting clean and widely distributed water droplet energy with high efficiency. However, the commonly used polymer films in TENGs for water droplet energy harvesting have the disadvantages of poor breathability, poor skin affinity, and irreparable hydrophobicity, which greatly hinder their wearable uses. Here, we report an all-fabric TENG (F-TENG), which not only has good air permeability and hydrophobic self-repairing properties but also shows effective energy conversion efficiency. The hydrophobic surface composed of SiO_2 nanoparticles and poly(vinylidenefluoride-*co*-hexafluoropropylene)/perfluorodecyltrichlorosilane (PVDF-HFP/FDTS) exhibits a static contact angle of 157° and displays excellent acid and alkali resistance. Because of its low glass transition temperature, PVDF-HFP can facilitate the movement of FDTS molecules to the surface layer under heating conditions, realizing hydrophobic self-repairing performance. Furthermore, with the optimized compositions and structure, the water droplet F-TENG shows 7-fold enhancement of output voltage compared with the conventional single-electrode mode TENG, and a total energy conversion efficiency of 2.9% is achieved. Therefore, the proposed F-TENG can be used in multifunctional wearable devices for raindrop energy harvesting.**

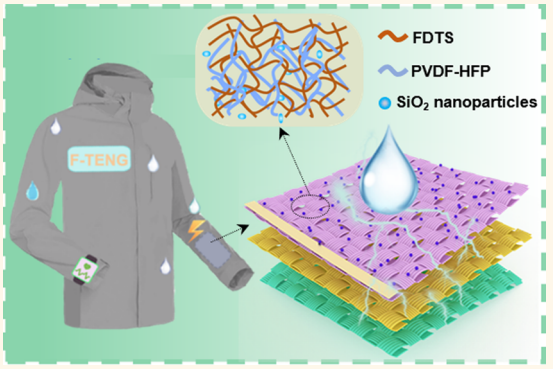

KEYWORDS: *fabric triboelectric nanogenerator, waterproof, hydrophobic, self-repairing, droplet energy harvesting*

INTRODUCTION

With the rapid development of human−machine interaction, health monitoring, and artificial intelligence, wearable technologies are thriving and have been successfully applied in virtual reality,[1] electric stimulation,[2] wearable digital healthcare,[3,4] *etc.*, which has inspired increasing interest in industry and the academic community. On the basis of these technologies, various multifunctional wearable devices have been created to serve humankind and greatly enrich our life.[5,6] Those wearable devices are widely distributed, and their special characteristics of portability, mobility, and being numerous and wireless makes them difficult to power by a conventional energy supply in a continuous manner.[7,8] At present, by harvesting the distributed mechanical energy around the wearable devices, some energy-harvesting technologies have been invented, such as the piezoelectric nanogenerator (PENG)[9] and triboelectric nanogenerator (TENG),[10] which provide a possible solution to solve the above problems. TENG, in particular, by coupling of contact electrification and electrostatic induction, has been considered as a potential solution to meet the energy demand in the new era of Internet of Things, with the merits of diverse choice of materials, low cost, high output, and even high efficiency in low frequency.[11] Overall, TENG can be seen as a feasible and promising strategy to effectively harvest low-frequency energy to power distributed wearable electronics.[12]

As one of the cleaning, renewable, and widely distributed energy sources, raindrop energy has low-frequency characteristics and has been demonstrated to be reasonably harvested by TENGs. This energy could help alleviate the energy crisis and is particularly suitable for powering distributed wearable electronics.[13] Extensive efforts have been devoted to harvest water droplet energy by TENGs.[14−19] The conventional works usually focus on the polymer films because of their good triboelectric performance with droplets, which cause poor breathability and discomfort for the human body for wearable

Received: August 13, 2021
Accepted: October 14, 2021
Published: October 20, 2021

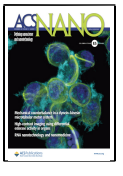

https://doi.org/10.1021/acsnano.1c06985
ACS Nano 2021, 15, 18172−18181

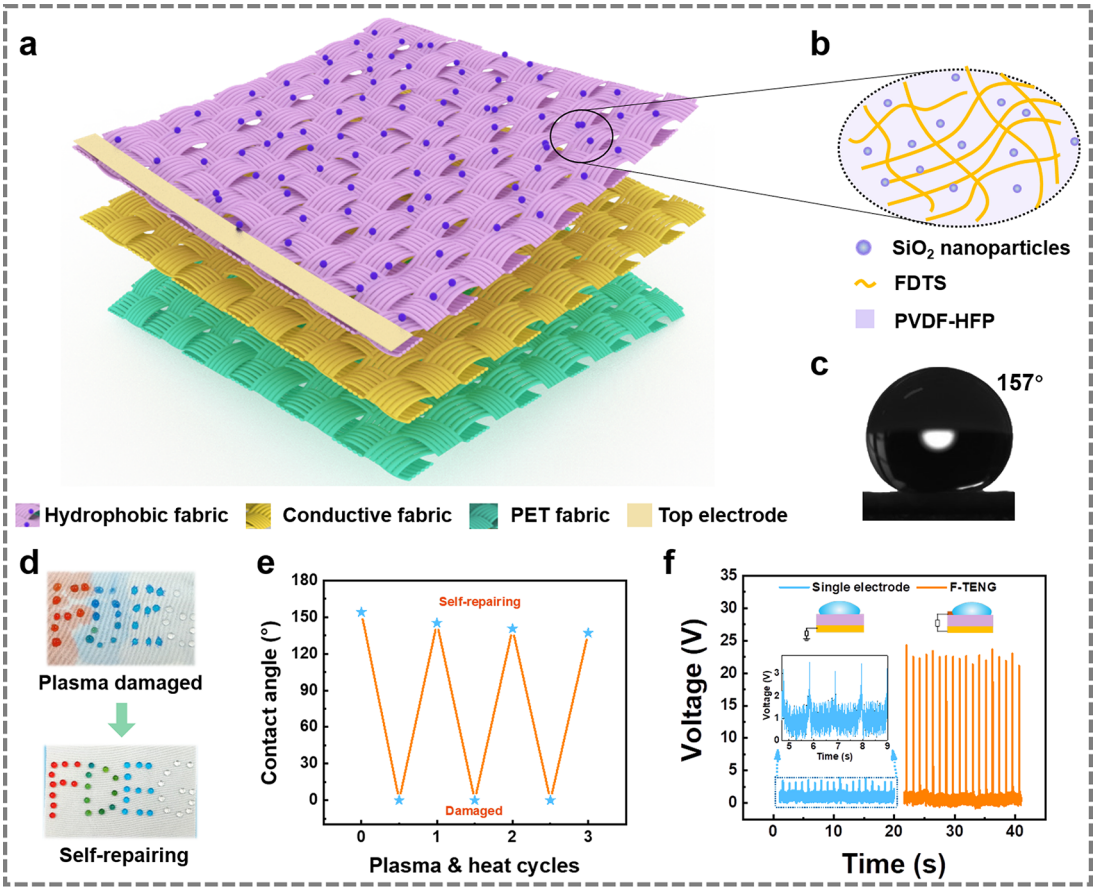

Figure 1. Features of the F-TENG. (a) Schematic diagram of the F-TENG. (b) Components of the hydrophobic surface. (c) Static contact angle of the hydrophobic fabric surface. (d) Photographs of the plasma damage and heat treatment of the hydrophobic fabric. (e) Contact angles of the hydrophobic fabric after plasma damage and heat treatment in several cycles (130 °C). (f) Comparison of output voltages between single-electrode mode TENG and the F-TENG for water droplet energy harvesting.

devices. Furthermore, common device structures for water droplet harvesting are either the single electrode mode or interdigital electrode structure mode, which possess a low charge utilization efficiency. To further achieve good separation between the droplet and the polymer film as well as improve the output performance of droplet energy harvesters, those chemical or physical processing methods, such as etching the polymer film by plasma,[20−24] introducing nanoparticles[23] and hydrophobic groups[16−18] on the polymer surface, are usually used to increase the hydrophobicity of polymers. Although these methods are effective for realizing good hydrophobicity, the construction of micro/nanostructures and hydrophobic groups on the polymer film surface is irrepairable. Once the micro/nanostructure and hydrophobic groups on the hydrophobic surface are damaged due to long-term physical abrasion, the performance of the hydrophobicity will decrease or even be destroyed. Therefore, it is an important research direction to find a new hydrophobic surface to solve the above problems of poor breathability, stretchability, and irreversible hydrophobicity of polymer films in wearable fields.

Fabrics with natural deformability, breathability, skin-friendliness, washability, and abrasion resistance can satisfy the above-mentioned requirements, showing great potential for application in wearable fields. Because of the hydrophilicity of common fabrics, many works have introduced hydrophobic groups to realize a hydrophobic fabric surface.[25−30] Recently, several works have employed hydrophobic fabrics for smart raincoats, umbrellas,[31] and tents[33] to harvest droplet energy for powering wearable electronics. For example, Xiong et al. reported an all-fabric-based dual-mode TENG with self-cleaning and antifouling properties to harvest both electrostatic energy and mechanical energy of droplets.[32] However, the hydrophobicity of these works is irreversible, which results in the short service lifetime of the device. Self-repairing properties can provide devices with longer service lifetime, lower repair costs, and higher safety levels, which is necessary for waterproof and self-cleaning wearable devices.[34−36] By introducing low-surface free energy components, hydrophobic self-repairing can be achieved by heating,[37,38] humidifying,[39] or UV light irradiation[40] to induce hydrophobic repair with the advantages of being simple, convenient, and fast. By integrating the hydrophobic reagent with elastomer or porous polymer realizing hydrophobic self-repair, the prepared hydrophobic surface can provide longer service life and increase the device safety.[38] Therefore, it is of great significance to exploit the multifunctional fabric not only with waterproof, breathable, and self-repairing characteristics but also realizing harvesting of human movement energy and environmental water droplet energy for sustainable powering wearable electronics.

Here, we report an all-fabric triboelectric nanogenerator (F-TENG) which not only has good air permeability, hydrophobicity, and self-repairing properties but also shows effective energy conversion efficiency. The hydrophobic fabric surface

https://doi.org/10.1021/acsnano.1c06985
ACS Nano 2021, 15, 18172−18181

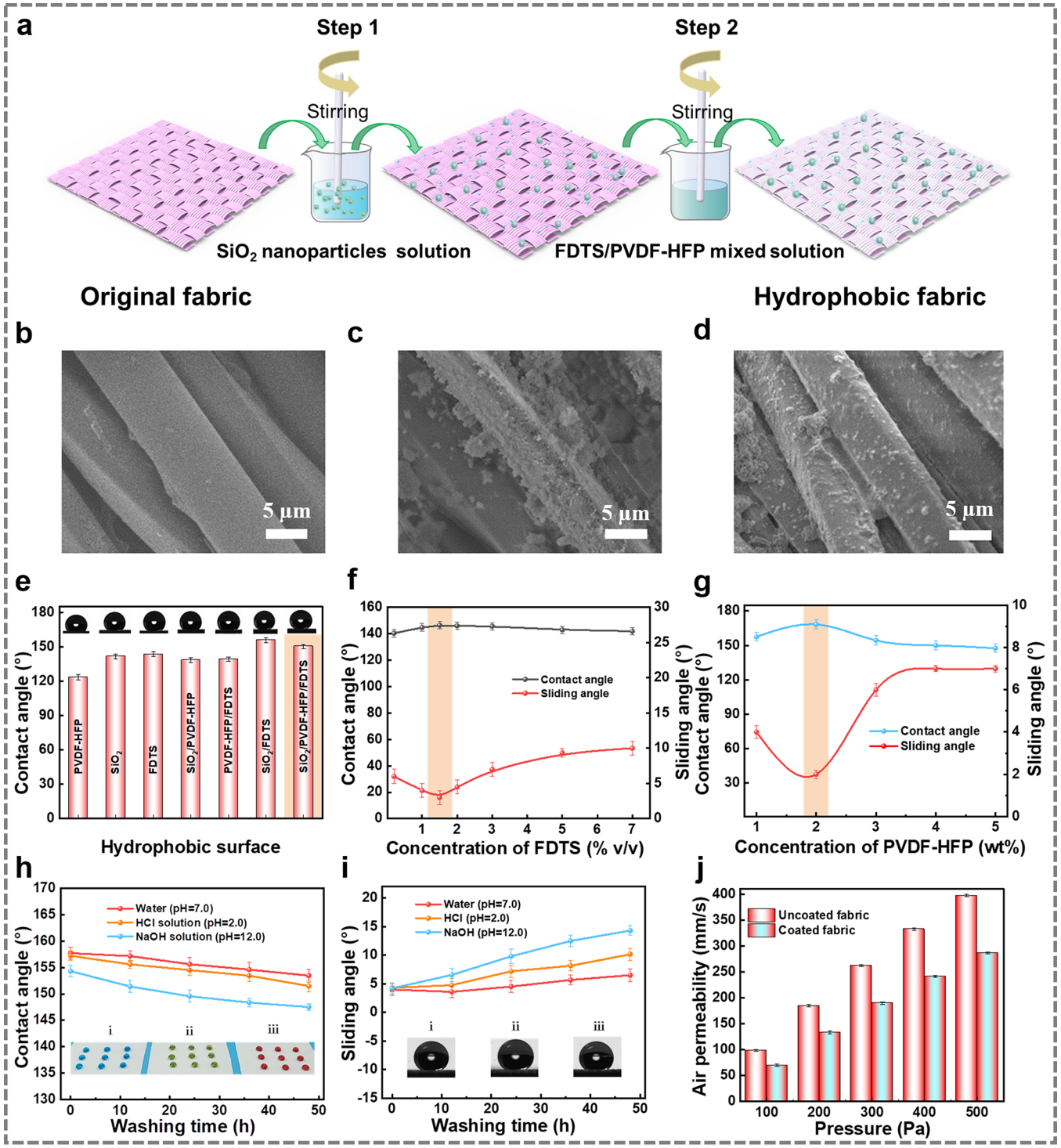

Figure 2. Preparation process and characterization of the hydrophobic fabric. (a) Preparation process of the hydrophobic fabric. (b) Surface morphology of the original fabric, (c) coated fabric with SiO_2 nanoparticles, and (d) the hydrophobic fabric. (e) Contact angle of the hydrophobic fabric with different components. Contact angle and sliding angle of the hydrophobic fabric at various concentrations of (f) FDTS and (g) PVDF-HFP. (h) Contact angle and (i) sliding angle of the hydrophobic fabric after several long-time washing (48 h) by deionized water, strong acid, and base solutions, respectively. (Insets show the photograph of the hydrophobic fabric washed by deionized water, HCl solution (pH = 2.0), and NaOH solution (pH = 12.0), respectively.) (j) Air permeability of the hydrophobic fabric at different pressures.

contains SiO_2 nanoparticles and a mixing coating of poly(vinylidenefluoride-*co*-hexafluoropropylene)/perfluorodecyltrichlorosilane (PVDF-HFP/FDTS) and displays the superhydrophobic characteristic with static contact angle of 157°, even showing excellent acid and alkali resistance. The SiO_2 nanoparticles increased surface roughness, and FDTS as a fluorosilane reagent mainly plays the roles of decreasing the surface free energy and increasing surface hydrophobicity. And PVDF-HFP endows the surface with hydrophobic self-repairing ability due to its thermoplastic's elastomer property.

https://doi.org/10.1021/acsnano.1c06985
ACS Nano 2021, 15, 18172−18181

Therefore, the mentioned three components work together to lower surface free energy and improve surface hydrophobicity and stability. The hydrophobic self-repairing properties can provide devices with longer service lifetime, lower repair costs, and higher safety levels, which are important for waterproof and self-cleaning wearable devices. Furthermore, the hydrophobic fabric was used for fabricating the F-TENG, and one water droplet can realize the output of 22 V and 7.5 nC with a totally energy conversion efficiency of 2.9%, which shows great potential applications in wearable water droplet energy harvesting, such as smart raincoats or umbrellas, for powering wearable electronics.

RESULTS AND DISCUSSION

Structural Features of the All-Fabric TENG. To improve the comprehensive performance of wearable devices and adapt the complex environment, multifunctional properties should be provided to wearable devices. We constructed a multifunctional fabric with self-cleaning, hydrophobic self-repairing, and anticorrosion properties and used it to fabricate the F-TENG for water droplet energy harvesting (Figure 1a). The detailed descriptions of the structure of F-TENG are as follows. The hydrophobic fabric surface is composed of SiO_2 nanoparticles, FDTS and PVDF-HFP (Figure 1b). Here, the three components work together to provide the original fabric surface hydrophobicity and lipophobicity, where SiO_2 nanoparticles increase surface roughness; FDTS largely decreases surface free energy and increases surface hydrophobicity; PVDF-HFP plays the roles in binding agent to immobilize the SiO_2 nanoparticles and FDTS polymer molecules and improve the durability of the hydrophobicity. The attained hydrophobic fabric of SiO_2/FDTS/PVDF-HFP can realize a super-hydrophobic property with a static contact angle (CA) of 157°, as shown in Figure 1c. Owing to its low glass transition temperature (T_g, −40 °C),[37] PVDF-HFP has a thermoplastic elastomer characteristic that facilitates the movement of FDTS polymer molecules in the coating layer and achieves hydrophobic self-repairing property. When the damaged hydrophobic surface is heated for several minutes or placed at room temperature for several hours, inside FDTS molecules of the coating layer will migrate to the damaged hydrophobic surface to lower the surface free energy and the surface hydrophobicity will recover again. The detailed mechanism of self-repair is explained in Note S1. The self-repairing ability of the hydrophobic coating was investigated by artificially damage the coated fabric with plasma treatment. As shown in Figure 1d,e, the hydrophobic surface was damaged and became hydrophilic by plasma treatment. When the plasma-treated fabric was heated for 10 min at 130 °C, the hydrophobicity would recover again. The self-repairing process is repeatable and the hydrophobic surface shows a slight decrease of the contact angle but still displays good hydrophobicity after several cycles. As shown in Figure 1e, the changes of contact angle by several plasma and heat treatments demonstrate the good hydrophobic self-repairing ability of the coated fabric. In addition, the hydrophobic self-repairing ability of the coated fabric can also be demonstrated at room temperature and higher temparature to accelerate the self-repairing process, whether the coated fabric is treated by abrasion or plasma treatment, as shown in Figure S1 and Note S2.

To further explore the potential of the hydrophobic fabric and achieve multifunctional applications, this hydrophobic fabric was fabricated as a wearable F-TENG for water droplet energy harvesting. As schematically illustrated in Figure 1a, the F-TENG is composed of three fabric layers and a top electrode, where the top electrode will directly contact with water droplet when the water droplet spreads on the hydrophobic surface. Here, the three fabric layers include top hydrophobic fabric, middle conductive fabric, and bottom original PET fabric. The bottom original PET fabric plays the roles in separating middle conductive fabric from human skin and protecting middle conductive fabric from external abrasion so as to reduce short circuit. When the F-TENG is applied for water droplet energy harvesting, it shows superior output performance compared with the conventional single-electrode mode TENG and even comparable to other water droplet energy harvester, as shown in Table S1. This attributes to the good triboelectric performance of this hydrophobic surface and the advantages of the recently reported TENG's structure.[41,42] As shown in Figure 1f and Figure S2 the electric output voltage and charge of the F-TENG have been improved about 7-fold compared with single-electrode mode TENG. The superhydrophobic property enables the water droplet to fully separate with the fabric surface to reduce the shielding effect by residual water droplets. The top electrode can make more electrostatic charges participate in charge transfer between the top electrode and middle conductive fabric and finally improve the electric output performance.

Preparation Process and Characterization of the Hydrophobic Fabric. The chemical structures of PVDF-HFP and FDTS are shown in Figure S3a, and the preparation process of the hydrophobic fabric is schematically illustrated in Figure 2a, which mainly contains a two-step dip-coating strategy. The corresponding chemistry characterization of preparation of the coated fabric has been discussed in Note S3. The cross-sectional SEM images of the coated fabric are shown in Figure S4. From the scanning electron microscope (SEM) images, we can know that silica nanoparticles can be uniformly distributed on the PET fabric surface and the coated PVDF-HFP/FDTS components seem commendably immobilizing the SiO_2 nanoparticles, which can enhance the hydrophobic stability of the coated fabric (Figure 2a−c). The fabric has been pretreated by NaOH solution to remove the surface impurity. As shown in Figure S5, the surface of the fabric pretreated by NaOH has little influence of the fabric surface morphography. Therefore, the SiO_2 particle plays a major role in increasing the surface roughness in our work. As shown in Figure S6a−c, the treated fabric not only has favorable hydrophobicity but also has good lipophobicity. Therefore, the hydrophobic fabric possesses a self-cleaning ability where the graphite powder can be easily removed from the hydrophobic surface by water droplet drip washing, while the untreated fabric was wetted and contaminated by the powders, as shown in Figure S6d.

Given that excellent hydrophobicity and stability are important factors to evaluate the performance of the hydrophobic layer, a series of experiments were conducted to optimize these properties. To enhance the performance of the hydrophobicity, stability, and self-repairing ability, the components of the hydrophobic coating layer and the concentration of each component are optimized. The surface morphology and functional groups are closely related with the hydrophobicity, which vary from different components. Here, the surfaces with SiO_2/FDTS and SiO_2/PVDF-HFP/FDTS have preferable hydrophobicity because SiO_2 particles can increase the surface roughness and FDTS provides low surface

https://doi.org/10.1021/acsnano.1c06985
ACS Nano 2021, 15, 18172−18181

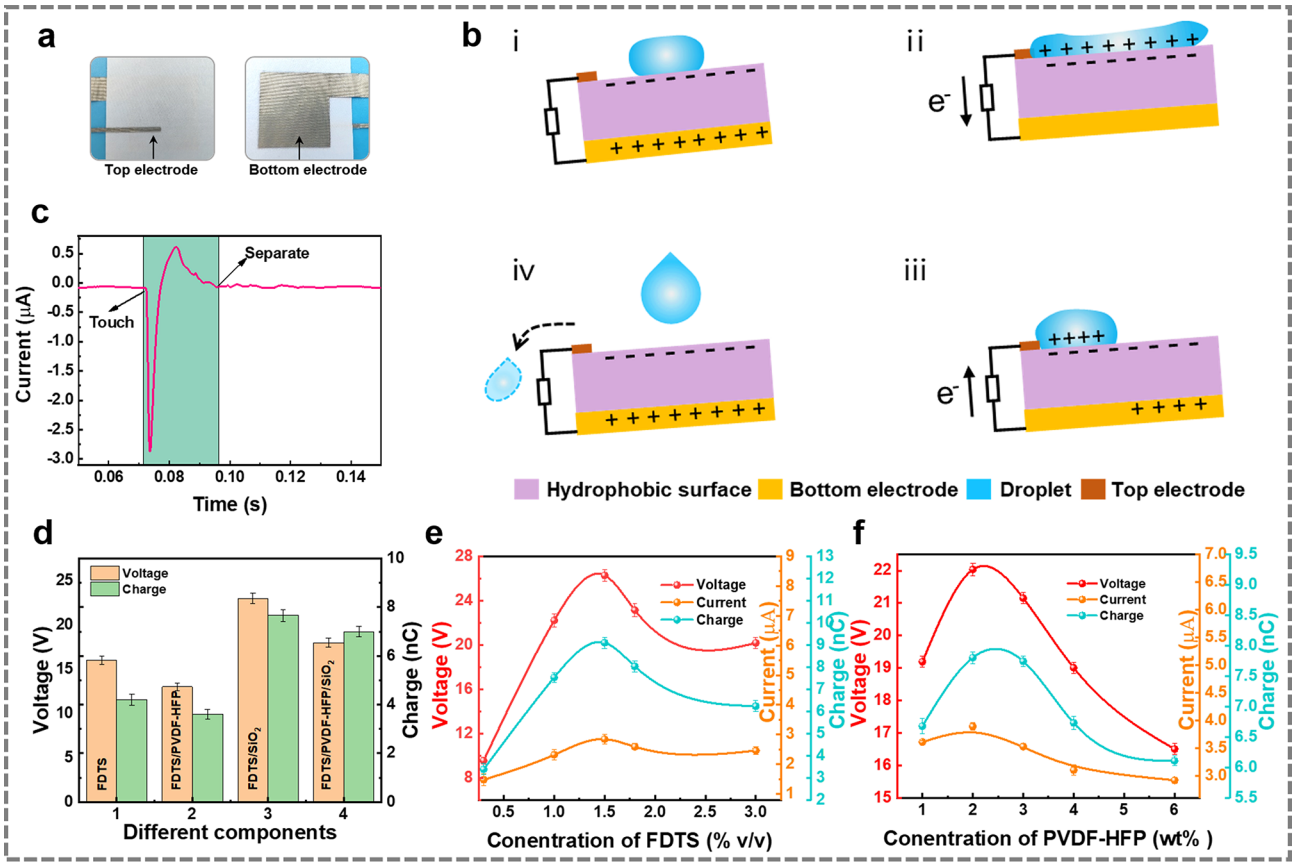

Figure 3. Working mechanism and optimization methods of the F-TENG. (a) Photograph of the F-TENG. (b) Working mechanism of the F-TENG. (c) Current signal generated by one water droplet. (d) Output voltage and charge of the hydrophobic fabric with different surface components, respectively. (e) Output voltage, current and charge of the hydrophobic fabric with various concentrations of FDTS, respectively. (f) Output voltage, current, and charge of the hydrophobic fabric with different concentrations of PVDF-HFP, respectively.

free energy, as shown in Figure 2e. Although the surface of SiO_2/FDTS has a better hydrophobic contact angle than the SiO_2/PVDF-HFP/FDTS surface, the SiO_2/FDTS surface shows poor hydrophobic stability. As shown in Figure S7, the contact angle of SiO_2/FDTS decreases from 156° to 101° after washing for 24 h with deionized water. In contrast, the SiO_2/PVDF-HFP/FDTS surface shows good hydrophobic stability as shown in the section of washing tests because the blinding agent of PVDF-HFP can immobilize the SiO_2 nanoparticles and FDTS molecules on the hydrophobic coating, as depicted in Figure 2d. In addition, the fluorine atom in the component of PVDF-HFP may helpful for the triboelectrification process.

Then we also optimized the concentration of FDTS and PVDF-HFP to further improve the combination performance of the hydrophobic surface. Considering that FDTS is the major contributor for favorable hydrophobicity due to its low surface free energy, it is considered first. As shown in Figure 2f, the surface hydrophobicity increases first and then decreases with the increases of FDTS concentration. The surface with a concentration of 1.5% (v/v) of FDTS has the largest contact angle and lowest sliding angle in our coating fabric. The contact angle will not endlessly increase with the increase of concentration of FDTS. Here, we choose 1.5% (v/v) as the optimal concentration of FDTS. In addition, given that PVDF-HFP plays roles in strengthening surface stability and providing surface self-repairing ability, its concentration also is one of the important optimization parameters. Since a low concentration of PVDF-HFP cannot immobilize SiO_2 nanoparticles while a high concentration of PVDF-HFP will hinder the air permeability of fabric, we chose 2 wt % of PVDF-HFP as the optimal concentration, which also possesses the optimal hydrophobicity, as shown in Figure 2g.

To show the excellent hydrophobic stability of the coated fabric, washing tests with deionized water, strong acid, and alkali corrosion have been executed. The coated fabric was immersed in deionized water and strong acid and alkali solution and continuously washed for 48 h under magnetic stirring conditions, respectively. After the coated fabric was washed in deionized water, HCl solution (pH = 2), and NaOH solution (pH = 12) for 48 h, the contact angle of the coated fabric only slightly decreased (Figure 2h) and the corresponding sliding angle slightly increased (Figure 2i), still displaying the fine hydrophobicity as shown in Figure S8. The SEM images of coated fabrics washed with HCl and NaOH also indicate that the surface of coated fabric has no obvious morphology changes after the strong acid and alkali solution washing (Figure S9), which demonstrate that the coated fabric can resist the corrosion of strong acid and alkali. In addition, after continuously washing 48 h, silica nanoparticles can be clearly observed and evenly distributed on the coating surface, as the SEM image in the Figure S10, which indicates that the nanoparticles are firmly immobilized on the fabric surface and the coated fabric has hydrophobic stability. Mechanical robustness is the major challenge for super-hydrophobic coatings and was also considered in this work. The tape

https://doi.org/10.1021/acsnano.1c06985
ACS Nano 2021, 15, 18172−18181

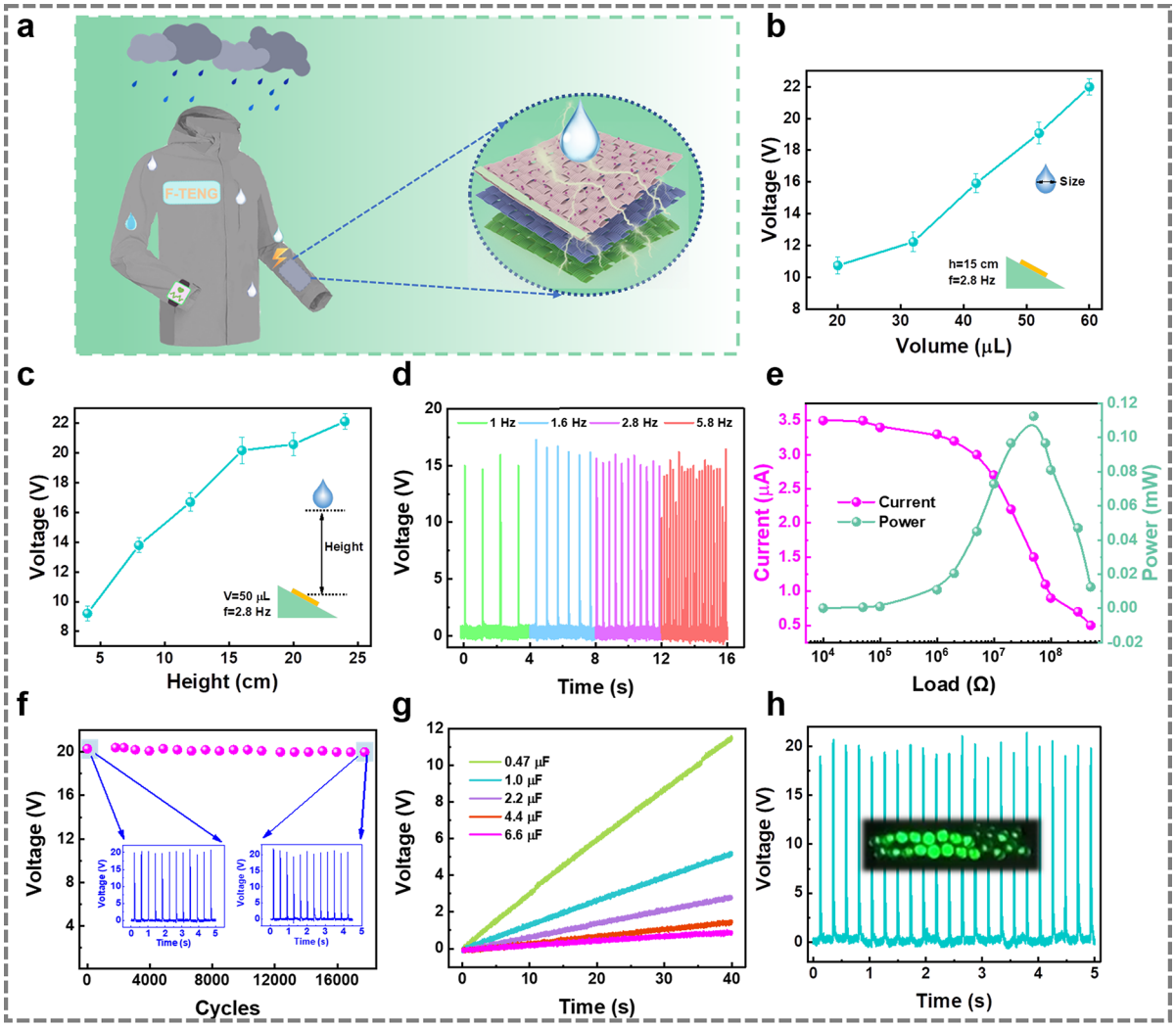

Figure 4. Applications of the F-TENG for water droplet energy harvesting. (a) Schematic diagram shows the application scenario of the F-TENG for wearable water droplet energy harvesting. (b) Output voltage of F-TENG with different volumes of water droplet. (c) Output voltage of F-TENG with water droplet at various dropping heights. (d) Output voltage of F-TENG with different dropping velocity of water droplet. (e) Output current and power of F-TENG with different external load resistances. (f) Electric output stability of F-TENG. (g) Charging curves of various capacitors charged by the F-TENG. (h) Electric output to power LED arrays (inset is the photographs of LED arrays powered by F-TENG).

peeling test and mechanical abrasion test were implemented to characterize the mechanical robustness of the coated fabric, which also demonstrates the favorable mechanical stability of the coated fabric (Figure S11 and Note S4). In addition, we also tested the air permeability of the coated fabric and the original fabric. As shown in Figure 2j, although the air permeability of the hydrophobic fabric has decreased a little bit compared with original fabric, the breathability of the hydrophobic fabric is still higher than commercial denim fabrics (~10 mm s^{-1}), and the breathability also increases with the increase of air pressure. These results show that the hydrophobic fabric still has good breathability and comfort in wearable application areas.

Working Mechanism and Optimization of F-TENG for Water Droplet Energy Harvesting. We have confirmed above that a favorable multifunctional hydrophobic fabric has been obtained. Furthermore, we used the multifunctional hydrophobic fabric to construct an F-TENG for water droplet power generation, as shown in Figure 3a. In combination with the latest research on water droplet energy harvesting, a special structure adopted in the device for water droplet energy harvesting, which introduced a top electrode on hydrophobic surface to periodic contact with water droplet.[40] The detailed working mechanism of the F-TENG is illustrated in Figure 3b. With droplets continually dripping on the hydrophobic surface, some negative charges will accumulate on the hydrophobic surface due to the contact electrification between hydrophobic surface and water droplets. Therefore, after several water droplets fall on the surface, a layer of stable triboelectric negative charges will distribute on the hydrophobic surface. Here, we only focus on the stable working cycles. The negative electrostatic charges on the surface of the hydrophobic layer will induce opposite charges in the bottom electrode (Figure 3b (i)). When the water droplet drips from a high location, the water droplet first drops on the surface and then spreads on the hydrophobic surface. Before the water droplet touches with the top electrode, all of the induced charges will distribute on the bottom electrode (Figure 3b (ii)). Once the spreading droplet touches with the top electrode, electrons will transfer from the top electrode to the bottom electrode to balance the potential

https://doi.org/10.1021/acsnano.1c06985
ACS Nano 2021, 15, 18172−18181

difference, generating a peak current signal as the negative current signal shown in Figure 3b (iii) and Figure 3c. After the spreading water droplet reaches the maximum area, the water droplet begins to contract and slide away from the hydrophobic surface. Since the spreading area of the water droplet decreases with the contract of the water droplet, opposite charges will be induced in the bottom electrode again for balancing the negative charges on the hydrophobic surface and a opposite peak current is generated, as shown by the positive current signal in Figure 3b (iv) and Figure 3c. Since the process of building the induced charges in the bottom electrode is in accordance with the water droplet shrinkage, the relaxing time of the signal is longer. When the water droplet slides away and does not contact the top electrode, the current signal will disappear. The corresponding voltage signal is shown in Figure S12. The explanation of the improvement of electric output performance is shown in Note S5.

Given that the surface layer with different components not only influences the surface hydrophobicity but also closely relates with the triboelectric performance, the electric output performance of each surface with different components and concentrations was also tested to obtain the optimal hydrophobic fabric surface. Since FDTS provides better hydrophobicity and the water droplets can slide off the surface, we chose the coated fabric with FDTS as the reference material and further investigated the effects of additives of PVDF-HFP, SiO_2, and SiO_2/PVDF-HFP on the electric performance of TENG. By comparing the electric output of the several coated fabrics with different components, the variation tendency of the voltage, current, and charge are consistent with the variation tendency of the hydrophobicity of the coated fabric in our experiment, respectively. The results show that the fabric surface with preferable hydrophobicity also has a better output performance. Since the surface has better hydrophobicity, water droplets can more easily and quickly slide away from surface without residual water droplet. The residual water droplet on the surface will shield a part of negative charges on dielectric, which decreases the number of induced charges on bottom electrode. In addition, since better hydrophobic surface allows droplets to quickly slide off the surface, which can achieve high-frequency water droplet energy harvesting and the surface with preferable hydrophobicity can harvest more droplet energy at per unit time and increase the total output power.[44] As shown in Figure 3d,g and Figure S13, hydrophobic fabrics with SiO_2/FDTS and SiO_2/PVDF-HFP/FDTS have the preferable electric output. Although the coated fabric containing SiO_2/FDTS possesses higher electric output than SiO_2/PVDF-HFP/FDTS, the coated fabric of SiO_2/FDTS has poor stability because the SiO_2/FDTS will shed from the coating layer without the immobilization of PVDF-HFP after a short time water droplet impact and gradually becomes hydrophilic (Figure S7). As shown in Figure S14, the output voltage decreases from 20 to 5 V after continuously working for 2 h, which shows the instability of the SiO_2/FDTS surface. Therefore, we chose the surface of SiO_2/PVDF-HFP/FDTS for the following study. According to Figure 3e with respect to the optimization of FDTS, it can be found that the surface with 1.5% (v/v) FDTS also has optimal electric output performance, which is consistent with the above contact angle change in the above optimization of FDTS concentration part, demonstrating that the better surface hydrophobicity tends to obtain the better electrical output performance again. In addition, the surface with 2 wt % of PVDF-HFP has the optimal electric output performance, as shown in Figure 3f.

Applications of the F-TENG for Water Droplet Energy Harvesting. To demonstrate the good performance of the F-TENG for water energy harvesting, a series of experiments are conducted to simulate the practical conditions to test the electric performance of the F-TENG (Figure 4a). The position, size, height, and impacting frequency of water droplets are systematically studied. Effects of water droplet positions on the output performance of F-TENG are detailed described in Figure S15 and Note S6. As shown in Figure 4b and Figure S11a, the output voltage increases with the increase of water droplet volume, which is attributed to the increased contact area of one water droplet on the hydrophobic surface. We chose the water droplet with a volume of 60 μL to execute the following study. As shown in Figure 4c and Figure S16b, the output voltage increases with the height of water droplet because the spreading area and the impact force between water droplet and hydrophobic surface increase with the water droplet height. It is supposed that a larger impact force will facilitate the electron transfer between the dielectric and water droplet because it is beneficial for electron cloud to overlap.[43] However, when the height reaches a certain value, the larger water droplet will split into much small droplets because of the droplet's Weber number increasing, which is harmful for the output performance. The detailed description of the effect of Weber number is shown in Note S7. Furthermore, the output voltage remains constant at different dropping velocity because the voltage has a positive proportional relationship with contact area, where the water droplet spread area keeps stable with the velocity of water droplet (Figure 4d). The maximum output power of the F-TENG is up to 0.11 mW with the external matched resistance of 50 MΩ, which is much higher than the conventional single electrode mode TENG and fabric-based TENG for water droplet energy harvesting (Figure 4e). A total energy conversion efficiency of 2.9% is achieved. The calculation of the energy conversion efficiency of F-TENG is shown in Note S8.

The electric output stability of the F-TENG was also studied. As shown in Figure 4f, after working for 18000 cycles, the output voltage of the F-TENG shows no noticeable fluctuation, indicating its long-term stability for application in practical water droplet energy harvesting. To further demonstrate the ability of the F-TENG for powering electronics, it is used for charging different commercial capacitors. As the charging curves shown in Figure 4g, the capacitor of 0.47 μF can be charged to 12 V and the capacitor of 6.6 μF can be charged to 0.9 V within 40 s. Finally, the F-TENG is used to light LEDs, and we find that one water droplet can light 25 LEDs (Movie S1), which demonstrates the F-TENG can effectively harvest water droplet energy for powering wearable electronics. The F-TENG can also combine with the contact-separation mode TENG for simultaneously harvesting the mechanical energy of human motion and water droplet energy, showing great potential for application in wearable fields.

CONCLUSIONS

In summary, an all-fabric TENG with good air permeability, hydrophobic self-repairing properties, and effective energy conversion efficiency is reported for water droplet energy harvesting. The hydrophobic fabric is prepared by successively coating SiO_2 nanoparticle solution and PVDF-HFP/FDTS

https://doi.org/10.1021/acsnano.1c06985
ACS Nano 2021, 15, 18172−18181

mixing solution. The deposited SiO_2 nanoparticles largely increase the surface roughness. The FDTS as a fluorosilane reagent mainly plays the roles in decreasing the surface free energy and increasing surface hydrophobicity, and PVDF-HFP plays the roles in binding agent to immobilize the SiO_2 nanoparticles and endowing the hydrophobic surface with self-repairing ability due to its thermoplastic's elastomer property. By optimizing the components and concentrations of each material, the prepared hydrophobic fabric shows favorable wash durability, resistant to acid and alkali corrosion, and hydrophobic self-repairing ability. Furthermore, the hydrophobic fabric as a wearable water droplet harvester can effectively convert water droplet energy into electric energy with the output of 22 V and 7.5 nC. The F-TENG with favorable air permeability, hydrophobic self-repairing, and higher conversion efficiency not only has comprehensive application prospects in multifunctional wearable devices but also can combine with the contact-separation mode TENG for simultaneously harvesting mechanical energy of human motion and water droplet energy.

EXPERIMENTAL SECTION

Materials. 1*H*,1*H*,2*H*,2*H*-Perfluorodecyltrichlorosilane (98%, Aladdin), poly(vinylidene fluoride-*co*-hexafluoropropylene) (M_w = 455,000, polydispersity = 4.12, Macklin), modified silica nanoparticles (50 nm, Shanghai Yuanjiang Chemical Co., Ltd.), dimethylformamide (99.5%, Yong Da Chemical), tetrahydrofuran (99.5%, Yong Da Chemical). Commercial polyester fabrics were plain weave, thickness = 343 μm.

Pretreatment of the Polyester Fabric. The commercial fabric was immersed in NaOH solution (1 mol L^{-1}) and magnetic stirred for 1 h at 60 °C to remove the impurities on the original fabric surface. Then the fabric was rinsed with deionized water to remove the residual alkali solution until the alkali was totally removed (pH = 7.0). Finally, the treated fabric was placed in an oven to dry with the temperature of 60 °C or dried in nature environment, and the pretreatment of original fabric is finished.

Preparation of Silica Nanoparticles Solution. The modified-hydrophobic silica nanoparticles of 1.5 g were added into the tetrahydrofuran (THF) solution of 31 mL at a temperature of 35 °C, and it was magnetically stirred until the silica nanoparticles were totally dispersed and a homogeneous solution was formed. The silica nanoparticle solution was prepared.

Preparation of PVDF-HFP/FDTS Solution. The PVDF-HFP/FDTS solution was prepared by mixing PVDF-HFP (1.0 g) and FDTS (0.75 mL) in DMF (50 mL) to form a homogeneous solution. After magnetic stirring for 0.5 h, the solution was prepared for coating on fabrics.

Preparation of the Hydrophobic Fabric. A two-step dip-coating method was used to treat the fabric. In the first step, the original fabric was immersed in the silica nanoparticles solution (silica nanoparticles concentration, 1.5 wt %) for 2 min to deposit silica nanoparticles on fabric surface. The treated fabric was then dried at room temperature for 15 min. Without any rinsing, the particle-coated fabric was immersed in the second coating solution for 2 min to deposit PVDF-HFP/FDTS on the surface. The coated fabric was finally dried at 130 °C for 1 h.

Fabrication of the F-TENG. A conductive fabric was taped on the back side of the hydrophobic SiO_2/PVDF-HFP/FTDS-coated fabric with dimensions of 3 cm × 3 cm as the bottom electrode. Another conductive fabric with dimensions of 3 cm × 0.5 cm was used as the top conductive wire. An original piece of fabric was tapped on the bottom layer to separate skin from the middle conductive fabric to avoid direct contact of the electrode with human skin. The middle conductive fabric and top conductive wire were connected by an external electric wire.

Plasma Treatment. The hydrophobic fabric was subjected to plasma treatment with Ar (50 sccm gas flow) and O_2 (5 sccm gas flow) as source gas to damage the fabric surface hydrophobic layer. For each plasma treatment, a 5 min plasma treatment under a power of 19 W was employed. Such a plasma treatment can make fabrics completely hydrophilic. The plasma-treated fabric was heated at 130 °C to recover initial hydrophobicity.

Acid and Base Stability. The hydrophobic fabric was immersed and stirred in strong acid solution (HCl, pH = 2) or base solution (NaOH, pH = 12) at room temperature for 48 h. The static contact angle and sliding angle were tested every 12 h of continuous washing.

Characterization and Electrical Measurements. A field-emission SEM (SU1510) was employed to characterize the micromorphology of the fabric surface. The static contact angle and sliding angle were measured by a video-based optical contact angle measuring system (Dataphysics OCA15 Pro) with water droplets of 7 μL. To measure the electric output of the TENG, a programmable electrometer (Keithley Instruments model 6514) was used.

ASSOCIATED CONTENT

Supporting Information

The Supporting Information is available free of charge at https://pubs.acs.org/doi/10.1021/acsnano.1c06985.

Figures S1−16: comparison of the coated fabric before and after abrasion; comparison of the output charge of F-TENG and single electrode mode TENG for water droplet energy harvesting; characterization of the coated fabric; cross-sectional SEM images of the coated fabric; SEM image of the original fabric and pretreated fabric by NaOH; characteristics of hydrophobic and self-cleaning property of the coated fabric; contact angle change of the FDTS/SiO_2 hydrophobic fabric; hydrophobicity of the coated fabric after long-time washing; SEM of the coated fabric after washing by strong acid and alkali solution; distribution of SiO_2 nanoparticles on the coated fabric after washing by water; mechanical tape-peeling and abrasion test; voltage signal of the F-TENG for water droplet energy harvesting; optimization directions of the F-TENG; stability of SiO_2/FDTS coated fabric TENG; output performance of the F-TENG when the droplet in different impacting positions; output voltages of the F-TENG at different conditions. Table S1: comparison of the water droplet energy conversion efficiency of the F-TENG with reported representative works (PDF)

Lighting LED process of the F-TENG for harvesting water droplet energy (MP4)

AUTHOR INFORMATION

Corresponding Authors

Kai Dong − *Beijing Institute of Nanoenergy and Nanosystems, Chinese Academy of Sciences, Beijing 101400, P. R. China; School of Nanoscience and Technology, University of Chinese Academy of Sciences, Beijing 100049, P. R. China;* orcid.org/0000-0001-6314-1546; Email: dongkai@binn.cas.cn

Zhong Lin Wang − *Beijing Institute of Nanoenergy and Nanosystems, Chinese Academy of Sciences, Beijing 101400, P. R. China; School of Nanoscience and Technology, University of Chinese Academy of Sciences, Beijing 100049, P. R. China; CUSPEA Institute of Technology, Wenzhou, Zhejiang 325024, P. R. China; School of Materials Science and Engineering, Georgia Institute of Technology, Atlanta,*

https://doi.org/10.1021/acsnano.1c06985
ACS Nano 2021, 15, 18172−18181

Georgia 30332-0245, United States; orcid.org/0000-0002-5530-0380; Email: zhong.wang@mse.gatech.edu

Authors

Cuiying Ye − *Beijing Institute of Nanoenergy and Nanosystems, Chinese Academy of Sciences, Beijing 101400, P. R. China; School of Nanoscience and Technology, University of Chinese Academy of Sciences, Beijing 100049, P. R. China*

Di Liu − *Beijing Institute of Nanoenergy and Nanosystems, Chinese Academy of Sciences, Beijing 101400, P. R. China; School of Nanoscience and Technology, University of Chinese Academy of Sciences, Beijing 100049, P. R. China*

Xiao Peng − *Beijing Institute of Nanoenergy and Nanosystems, Chinese Academy of Sciences, Beijing 101400, P. R. China; School of Nanoscience and Technology, University of Chinese Academy of Sciences, Beijing 100049, P. R. China*

Yang Jiang − *Beijing Institute of Nanoenergy and Nanosystems, Chinese Academy of Sciences, Beijing 101400, P. R. China; School of Nanoscience and Technology, University of Chinese Academy of Sciences, Beijing 100049, P. R. China*

Renwei Cheng − *Beijing Institute of Nanoenergy and Nanosystems, Chinese Academy of Sciences, Beijing 101400, P. R. China; School of Nanoscience and Technology, University of Chinese Academy of Sciences, Beijing 100049, P. R. China*

Chuan Ning − *Beijing Institute of Nanoenergy and Nanosystems, Chinese Academy of Sciences, Beijing 101400, P. R. China; School of Nanoscience and Technology, University of Chinese Academy of Sciences, Beijing 100049, P. R. China*

Feifan Sheng − *Beijing Institute of Nanoenergy and Nanosystems, Chinese Academy of Sciences, Beijing 101400, P. R. China; School of Chemistry and Chemical Engineering, Guangxi University, Nanning 530004, P. R. China*

Yihan Zhang − *Beijing Institute of Nanoenergy and Nanosystems, Chinese Academy of Sciences, Beijing 101400, P. R. China; School of Nanoscience and Technology, University of Chinese Academy of Sciences, Beijing 100049, P. R. China*

Complete contact information is available at: https://pubs.acs.org/10.1021/acsnano.1c06985

Author Contributions

$^{\delta}$C.Y., D.L., and X.P. contributed equally to this work.

Notes

The authors declare no competing financial interest.

ACKNOWLEDGMENTS

The authors are grateful for the support received from the National Natural Science Foundation of China (Grant No. 22109012), Natural Science Foundation of the Beijing Municipality (Grant No. 2212052), and the Fundamental Research Funds for the Central Universities (Grant No. E1E46805).

REFERENCES

(1) Sun, Z.; Zhu, M.; Zhang, Z.; Chen, Z.; Shi, Q.; Shan, X.; Yeow, R. C. H.; Lee, C. Artificial Intelligence of Things (AIoT) Enabled Virtual Shop Applications Using Self-Powered Sensor Enhanced Soft Robotic Manipulator. *Adv. Sci.* **2021**, *8* (14), No. e2100230.

(2) Yu, J. R.; Gao, G. Y.; Huang, J. R.; Yang, X. X.; Han, J.; Zhang, H.; Chen, Y. H.; Zhao, C. L.; Sun, Q. J.; Wang, Z. L. Contact-Electrification-Activated Artificial Afferents at Femtojoule Energy. *Nat. Commun.* **2021**, *12* (1), 1581.

(3) Meng, K.; Zhao, S.; Zhou, Y.; Wu, Y.; Zhang, S.; He, Q.; Wang, X.; Zhou, Z.; Fan, W.; Tan, X.; Yang, J.; Chen, J. A Wireless Textile-Based Sensor System for Self-Powered Personalized Health Care. *Matter* **2020**, *2* (4), 896−907.

(4) Peng, X.; Dong, K.; Ning, C. A.; Cheng, R. W.; Yi, J.; Zhang, Y. H.; Sheng, F. F.; Wu, Z. Y.; Wang, Z. L. All-Nanofiber Self-Powered Skin-Interfaced Real-Time Respiratory Monitoring System for Obstructive Sleep Apnea-Hypopnea Syndrome Diagnosing. *Adv. Funct. Mater.* **2021**, *31*, 2103559.

(5) Peng, X.; Dong, K.; Ye, C.; Jiang, Y.; Zhai, S.; Cheng, R.; Liu, D.; Gao, X.; Wang, J.; Wang, Z. L. A Breathable, Biodegradable, Antibacterial, and Self-Powered Electronic Skin Based on All-Nanofiber Triboelectric Nanogenerators. *Sci. Adv.* **2020**, *6* (26), No. eaba9624.

(6) Jiang, Y.; Dong, K.; An, J.; Liang, F.; Yi, J.; Peng, X.; Ning, C.; Ye, C.; Wang, Z. L. UV-Protective, Self-Cleaning, and Antibacterial Nanofiber-Based Triboelectric Nanogenerators for Self-Powered Human Motion Monitoring. *ACS Appl. Mater. Interfaces* **2021**, *13* (9), 11205−11214.

(7) Dong, K.; Hu, Y.; Yang, J.; Kim, S.-W.; Hu, W.; Wang, Z. L. Smart Textile Triboelectric Nanogenerators: Current Status and Perspectives. *MRS Bull.* **2021**, *46*, 512−521.

(8) Dong, K.; Peng, X.; Wang, Z. L. Fiber/Fabric-Based Piezoelectric and Triboelectric Nanogenerators for Flexible/Stretchable and Wearable Electronics and Artificial Intelligence. *Adv. Mater.* **2020**, *32* (5), No. e1902549.

(9) Cao, X. L.; Xiong, Y.; Sun, J.; Zhu, X. X.; Sun, Q. J.; Wang, Z. L. Piezoelectric Nanogenerators Derived Self-Powered Sensors for Multifunctional Applications and Artificial Intelligence. *Adv. Funct. Mater.* **2021**, *31*, 2102983.

(10) Wang, Z. L. From Contact-Electrification to Triboelectric Nanogenerators. *Rep. Prog. Phys.* **2021**, *84*, 096502.

(11) Zi, Y.; Guo, H.; Wen, Z.; Yeh, M. H.; Hu, C.; Wang, Z. L. Harvesting Low-Frequency (<5 Hz) Irregular Mechanical Energy: A Possible Killer Application of Triboelectric Nanogenerator. *ACS Nano* **2016**, *10* (4), 4797−805.

(12) Wang, Z. L. Triboelectric Nanogenerator (TENG)-Sparking an Energy and Sensor Revolution. *Adv. Energy Mater.* **2020**, *10* (17), 2000137.

(13) Dong, K.; Peng, X.; An, J.; Wang, A. C.; Luo, J.; Sun, B.; Wang, J.; Wang, Z. L. Shape Adaptable and Highly Resilient 3D Braided Triboelectric Nanogenerators as E-Textiles for Power and Sensing. *Nat. Commun.* **2020**, *11* (1), 2868.

(14) Jiang, D.; Su, Y.; Wang, K.; Wang, Y.; Xu, M.; Dong, M.; Chen, G. A Triboelectric and Pyroelectric Hybrid Energy Harvester for Recovering Energy from Low-Grade Waste Fluids. *Nano Energy* **2020**, *70*, 104459.

(15) Chen, Y.; Kuang, Y.; Shi, D.; Hou, M.; Chen, X.; Jiang, L.; Gao, J.; Zhang, L.; He, Y.; Wong, C. P. A Triboelectric Nanogenerator Design for Harvesting Environmental Mechanical Energy from Water Mist. *Nano Energy* **2020**, *73*, 104765.

(16) Chen, X.; Xiong, J.; Parida, K.; Guo, M.; Wang, C.; Wang, C.; Li, X.; Shao, J.; Lee, P. S. Transparent and Stretchable Bimodal Triboelectric Nanogenerators with Hierarchical Micro-Nanostructures for Mechanical and Water Energy Harvesting. *Nano Energy* **2019**, *64*, 103904.

(17) Nie, S.; Guo, H.; Lu, Y.; Zhuo, J.; Mo, J.; Wang, Z. L. Superhydrophobic Cellulose Paper-Based Triboelectric Nanogenerator for Water Drop Energy Harvesting. *Adv. Mater. Technol.* **2020**, *5* (9), 52000454.

(18) Yang, L.; Wang, Y.; Guo, Y.; Zhang, W.; Zhao, Z. Robust Working Mechanism of Water Droplet-Driven Triboelectric Nanogenerator: Triboelectric Output *versus* Dynamic Motion of Water Droplet. *Adv. Mater. Interfaces* **2019**, *6* (24), 1901547.

(19) Wang, Y.; Gao, S.; Xu, W.; Wang, Z. Nanogenerators with Superwetting Surfaces for Harvesting Water/Liquid Energy. *Adv. Funct. Mater.* **2020**, *30* (26), 1908252.
(20) Liu, X.; Yu, A.; Qin, A.; Zhai, J. Highly Integrated Triboelectric Nanogenerator for Efficiently Harvesting Raindrop Energy. *Adv. Mater. Technol.* **2019**, *4* (11), 1900608.
(21) Lin, Z. H.; Cheng, G.; Lee, S.; Pradel, K. C.; Wang, Z. L. Harvesting Water Drop Energy by a Sequential Contact-Electrification and Electrostatic-Induction Process. *Adv. Mater.* **2014**, *26* (27), 4690−4696.
(22) Zhong, W.; Xu, L.; Zhan, F.; Wang, H.; Wang, F.; Wang, Z. L. Dripping Channel Based Liquid Triboelectric Nanogenerators for Energy Harvesting and Sensing. *ACS Nano* **2020**, *14* (8), 10510−10517.
(23) Lin, Z. H.; Cheng, G.; Wu, W. Z.; Pradel, K. C.; Wang, Z. L. Dual-Mode Triboelectric Nanogenerator for Harvesting Water Energy and as a Self-Powered Ethanol Nanosensor. *ACS Nano* **2014**, *8* (6), 6440−6448.
(24) Jin, S.; Wang, Y.; Motlag, M.; Gao, S.; Xu, J.; Nian, Q.; Wu, W.; Cheng, G. J. Large-Area Direct Laser-Shock Imprinting of a 3D Biomimic Hierarchical Metal Surface for Triboelectric Nanogenerators. *Adv. Mater.* **2018**, *30* (11), 1705840.
(25) Zhang, J.; Zhao, J.; Qu, W.; Wang, Z. Fabrication of Superhydrophobic Fabrics with Outstanding Self-Healing Performance in Sunlight. *Mater. Chem. Front.* **2019**, *3* (7), 1341−1348.
(26) Xi, G.; Fan, W.; Wang, L.; Liu, X.; Endo, T. Fabrication of Asymmetrically Superhydrophobic Cotton Fabrics *via* Mist Copolymerization of 2,2,2-Trifluoroethyl Methacrylate. *J. Polym. Sci., Part A: Polym. Chem.* **2015**, *53* (16), 1862−1871.
(27) Xue, C. H.; Fan, Q. Q.; Guo, X. J.; An, Q. F.; Jia, S. T. Fabrication of Superhydrophobic Cotton Fabrics by Grafting of POSS-Based Polymers on Fibers. *Appl. Surf. Sci.* **2019**, *465*, 241−248.
(28) Zhou, H.; Wang, H.; Niu, H.; Gestos, A.; Wang, X.; Lin, T. Fluoroalkyl Silane Modified Silicone Rubber/Nanoparticle Composite: A Super Durable, Robust Superhydrophobic Fabric Coating. *Adv. Mater.* **2012**, *24* (18), 2409−2412.
(29) Lim, H. S.; Baek, J. H.; Park, K.; Shin, H. S.; Kim, J.; Cho, J. H. Multifunctional Hybrid Fabrics with Thermally Stable Superhydrophobicity. *Adv. Mater.* **2010**, *22* (19), 2138−2141.
(30) Deng, B.; Cai, R.; Yu, Y.; Jiang, H.; Wang, C.; Li, J.; Li, L.; Yu, M.; Li, J.; Xie, L.; Huang, Q.; Fan, C. Laundering Durability of Superhydrophobic Cotton Fabric. *Adv. Mater.* **2010**, *22* (48), 5473−5477.
(31) Kwon, S. H.; Kim, W. K.; Park, J.; Yang, Y.; Yoo, B.; Han, C. J.; Kim, Y. S. Fabric Active Transducer Stimulated by Water Motion for Self-Powered Wearable Device. *ACS Appl. Mater. Interfaces* **2016**, *8* (37), 24579−84.
(32) Xiong, J.; Lin, M.-F.; Wang, J.; Gaw, S. L.; Parida, K.; Lee, P. S. Wearable All-Fabric-Based Triboelectric Generator for Water Energy Harvesting. *Adv. Energy Mater.* **2017**, *7* (21), 1701243.
(33) Lai, Y. C.; Hsiao, Y. C.; Wu, H. M.; Wang, Z. L. Waterproof Fabric-Based Multifunctional Triboelectric Nanogenerator for Universally Harvesting Energy from Raindrops, Wind, and Human Motions and as Self-Powered Sensors. *Adv. Sci.* **2019**, *6* (5), 1801883.
(34) Wang, H.; Xue, Y.; Ding, J.; Feng, L.; Wang, X.; Lin, T. Durable, Self-Healing Superhydrophobic and Superoleophobic Surfaces from Fluorinated-Decyl Polyhedral Oligomeric Silsesquioxane and Hydrolyzed Fluorinated Alkyl Silane. *Angew. Chem.* **2011**, *123* (48), 11635−11638.
(35) Li, Y.; Li, L.; Sun, J. Bioinspired Self-Healing Superhydrophobic Coatings. *Angew. Chem., Int. Ed.* **2010**, *49* (35), 6129.
(36) Kuroki, H.; Tokarev, I.; Nykypanchuk, D.; Zhulina, E.; Minko, S. Stimuli-Responsive Materials with Self-Healing Antifouling Surface *via* 3D Polymer Grafting. *Adv. Funct. Mater.* **2013**, *23* (36), 4593−4600.
(37) Zhou, H.; Wang, H.; Niu, H.; Zhao, Y.; Xu, Z.; Lin, T. A Waterborne Coating System for Preparing Robust, Self-Healing, Superamphiphobic Surfaces. *Adv. Funct. Mater.* **2017**, *27* (14), 1604261.
(38) Zhou, H.; Wang, H.; Niu, H.; Gestos, A.; Lin, T. Robust, Self-Healing Superamphiphobic Fabrics Prepared by Two-Step Coating of Fluoro-Containing Polymer, Fluoroalkyl Silane, and Modified Silica Nanoparticles. *Adv. Funct. Mater.* **2013**, *23* (13), 1664−1670.
(39) Wu, G.; An, J. L.; Tang, X. Z.; Xiang, Y.; Yang, J. L. A Versatile Approach towards Multifunctional Robust Microcapsules with Tunable, Restorable, and Solvent-Proof Superhydrophobicity for Self-Healing and Self-Cleaning Coatings. *Adv. Funct. Mater.* **2014**, *24* (43), 6751−6761.
(40) Cong, Y.; Chen, K. L.; Zhou, S. X.; Wu, L. M. Synthesis of pH and UV Dual-Responsive Microcapsules with High Loading Capacity and Their Application in Self-Healing Hydrophobic Coatings. *J. Mater. Chem. A* **2015**, *3* (37), 19093−19099.
(41) Xu, W.; Zheng, H.; Liu, Y.; Zhou, X.; Zhang, C.; Song, Y.; Deng, X.; Leung, M.; Yang, Z.; Xu, R. X.; Wang, Z. L.; Zeng, X. C.; Wang, Z. A Droplet-Based Electricity Generator with High Instantaneous Power Density. *Nature* **2020**, *578* (7795), 392−396.
(42) Wu, H.; Mendel, N.; van der Ham, S.; Shui, L.; Zhou, G.; Mugele, F. Charge Trapping-Based Electricity Generator (CTEG): An Ultrarobust and High Efficiency Nanogenerator for Energy Harvesting from Water Droplets. *Adv. Mater.* **2020**, *32* (33), No. e2001699.
(43) Xu, C.; Zi, Y. L.; Wang, A. C.; Zou, H. Y.; Dai, Y. J.; He, X.; Wang, P. H.; Wang, Y. C.; Feng, P. Z.; Li, D. W.; Wang, Z. L. On the Electron-Transfer Mechanism in the Contact-Electrification Effect. *Adv. Mater.* **2018**, *30* (15), 1706790.
(44) Wang, L.; Song, Y.; Xu, W.; Li, W.; Jin, Y.; Gao, S.; Yang, S.; Wu, C.; Wang, S.; Wang, Z. Harvesting Energy from High-Frequency Impinging Water Droplets by a Droplet-Based Electricity Generator. *EcoMat* **2021**, *3* (4), No. e12116.

https://doi.org/10.1021/acsnano.1c06985
ACS Nano 2021, 15, 18172−18181